Turk J Elec Engin, VOL.15, NO.2 2007, © TÜBİTAK

Modelling a Deposition Process in Collective Construction

Robert L. STEWART, R. Andrew RUSSELL and Lindsay KLEEMAN
Centre for Perceptive and Intelligent Machines in Complex Environments: Intelligent Robotics
Monash University, Wellington Rd, Clayton, VIC 3800, AUSTRALIA
e-mail: RLStewart@ieee.org • Andy.Russell@eng.monash.edu.au and
e-mail: Lindsay.Kleeman@eng.monash.edu.au

Abstract

During collective construction tasks, swarm robots coordinate their actions in space and time to build structures that conform to some given design or specification. In this paper, a simulation model and a mathematical model (based on a Markov chain) are introduced to describe the deposition process of a previously detailed robotic swarm system that uses templates and feedback to facilitate construction. The models are based on the behaviour and geometry of real robots and predict the dynamics observed during practical trials as well as explaining the occurrence of different spatial patterns of building blocks. Furthermore, the models provide an insight into the swarm system and a solid basis for understanding the feedback mechanism that is fundamental to its operation. The theoretical models are verified with practical trials performed by physical robots.

1. Introduction

Social insect colonies have been described by some researchers as superorganisms – single entities composed of many distributed autonomous parts [1, 2]. While these parts may be relatively simple, there emerges a collective or swarm intelligence, manifest in the global and collective tasks performed.

Swarm robotics is a flourishing field of research that draws inspiration from social insects and other animal societies and applies the principles learnt to the design of multi-robot systems [3]. Many problem domains in the field have been investigated, all of which study some aspect of "how collectively intelligent behavior can emerge from [the] local interactions of a large number of relatively simple physically embodied agents" [4]. Problem domains investigated include: foraging, clustering, sorting, box-pushing, stick pulling, exploration, formation and congregation forming, collective relocation and collective construction (for a review of these areas see [5]). Solutions to such problems have demonstrated the power of the swarm intelligence paradigm.

Whilst numerous swarm robotic systems have been detailed, there is still a need for more work regarding their analysis and modelling along the lines of [6–10]. In this paper, simulation and mathematical models are introduced to describe the deposition process of a particular robotic swarm system capable of collective construction. The models successfully capture the dynamics evident in practical trials as well as providing some scope for making predictions. Most importantly, the models allow for a deeper understanding

of the swarm system giving a solid basis for understanding why it functions successfully.

The remainder of this paper is organised as follows. In Section 2 a brief review of the collective construction problem domain is provided. The section also includes details of previous work regarding the swarm system modelled in this paper. Sections 3 and 4 then introduce the simulation and mathematical models respectively. These were developed to describe the deposition process under study. Finally, Section 5 provides a general discussion and conclusion for the paper.

2. Background Information: Collective Construction

In the collective construction problem domain, researchers investigate how best to design robot swarms capable of building structures that conform to some given pattern or specification. This requires that swarm members coordinate their actions in both space and time in order for a coherent structure to be built [11]. Requiring the design of the robots to remain within the swarm paradigm makes construction problems even harder; since, not only must coordination be achieved, but it must be done without a map, without knowledge of a global coordinate system and without global radio communications or explicitly shared memory.

A number of works have developed techniques for building structures of a specific shape. Inspired by ants, Melhuish, Welsby, Edwards [12] showed how linear walls could be built by robots, using preplaced templates (patterns). Wawerla, Sukhatme, Matarić [13] developed an alternative approach to building linear walls with robots attaching coloured blocks to a preplaced seed block. Parker, Zhang, Ronald Kube [9] demonstrated the construction of circular nests by robots using a blind bulldozing algorithm similar to that observed in ants. Simulations by Welfel [14] revealed how arbitrary structures with non-crossing walls could be built using a leader robot and a radio communications system.

Recently, interest has turned towards the development of more general approaches to collective construction that allow a larger set of structures to be built. Most of the approaches make use of stigmergy[1], first introduced by Grassé [16], or similar mechanisms to coordinate construction. For example, Jones, Matarić [17] and Li, Zhang [18] have shown in simulation how self-assembling robots might attach to one another to form relatively complex structures. To do this, robots need only observe the local configuration and state of their neighbours. In the self-assembling system of Bishop et al. [19], a graph grammar is applied for the creation of certain shapes. Again, the robots in this system only attach to the formative structure when certain local conditions are met. Werfel, Bar-Yam, Nagpal [20] have proposed an alternative approach to construction in which robots move around a formative structure and request permission to attach a block. The authorisation to make the attachment is given by blocks already in the structure which maintain a map and communicate with each other.

To build complex structures, most researchers have required the use of relatively sophisticated building material and/or robots in order to enforce the global emergence of a desired structure. However, as we have previously shown, it is possible to build complex structures using only inert and homogeneous building material and minimalist robots [21–24]. Because the total system is minimalist it is, as a result, inexpensive and amenable to miniaturisation. Our approach has relied on the use of spatio-temporal varying templates or patterns that vary in space and with time, originally inspired by the simple template mechanism often used by social insects during construction [25, 26].

Figure 1 shows a photograph of the swarm with major hardware components labeled and Figure 2

[1] Stigmergy, a form of sematectonic communication, is "the guidance of work performed by social insects through the evidences of work previously accomplished" [15].

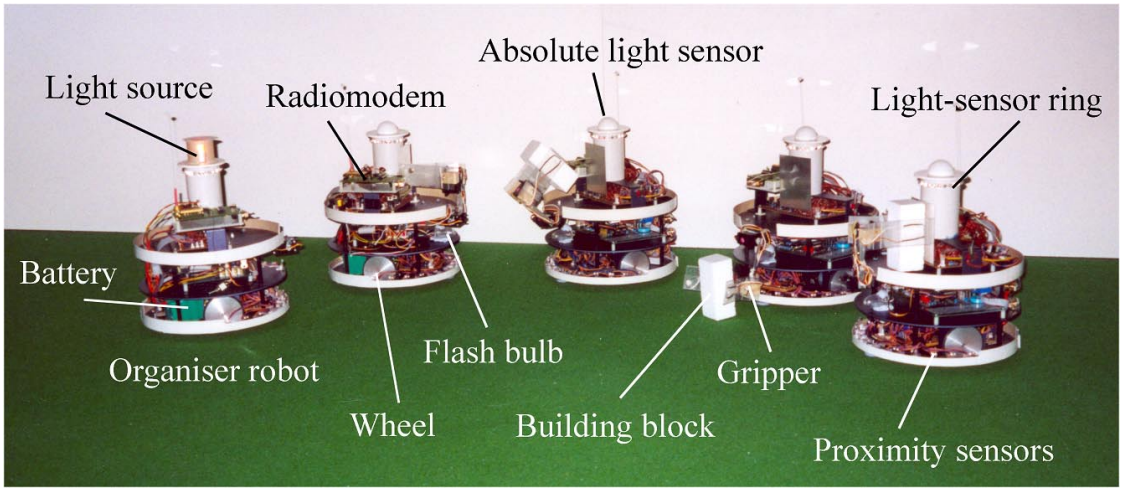

Figure 1. *The Robotermites*: a small 5-member swarm containing an organiser robot and 4 builder robots.

provides a schematic view of the robot subsystems. Each robot possessed a M16C/62 microcontroller, an array of infra-red (IR) proximity sensors for detecting objects, a light-sensor ring for detecting directional light intensity information and, a radiomodem for experiment initialisation and data logging purposes. Mobility was provided by two wheels that allowed rotation around the centre-point of the chassis. Stability was achieved when one of two diametrically opposed teflon pads made contact with the ground. Builder robots also had a gripper for picking up and putting down building blocks. The gripper was equipped with a magnet and reed switch that allowed the robot to sense if a block was being held. Additionally the builder robots had an absolute light sensor for detecting light intensity[2] and, a flash bulb for producing bursts of high intensity light. The organiser robot instead carried a light projector arranged to radiate light in a beam of 30 ° width.

The light source carried by the organiser robot creates a directional light-field gradient. By moving the light source and/or varying its intensity at each step in a recipe, a spatio-temporal varying template is produced. Builder robots respond to the light and deposit building material in a fixed window of light intensity called the deposition window. Through this process, the structure encoded in the recipe is built. A methodical approach to the formulation of the recipe has been detailed [5], that, in conjunction with the builder robots' behaviour, ensures spatio-temporal coordination during construction.

One important component of the demonstrated system was a distributed feedback mechanism that regulated construction under different environment and system conditions [24]. During a step in the construction recipe, builder robots attempt to access the deposition window in order to make a deposit. When they are unable to do this they become frustrated and produce a flash of light, which the organiser robot detects. On detecting a certain number of flash signals (*flash_count_max*), the organiser robot deems the current deposition window complete and then goes on to the next step in its recipe, creating a new deposition window. A setup for one of the practical experiments described in [24] is shown in Figure 3. The actual rule sets used by the organiser and builder robots are given in Rule Sets 1 and 2 respectively. Whilst the rule sets were implemented as sequential programs, they could just as readily have be implemented using

[2]Calibration of each builder robot's absolute light sensor was necessary to ensure they all had a consistent quantifiable response to light (see [5, 24] for details).

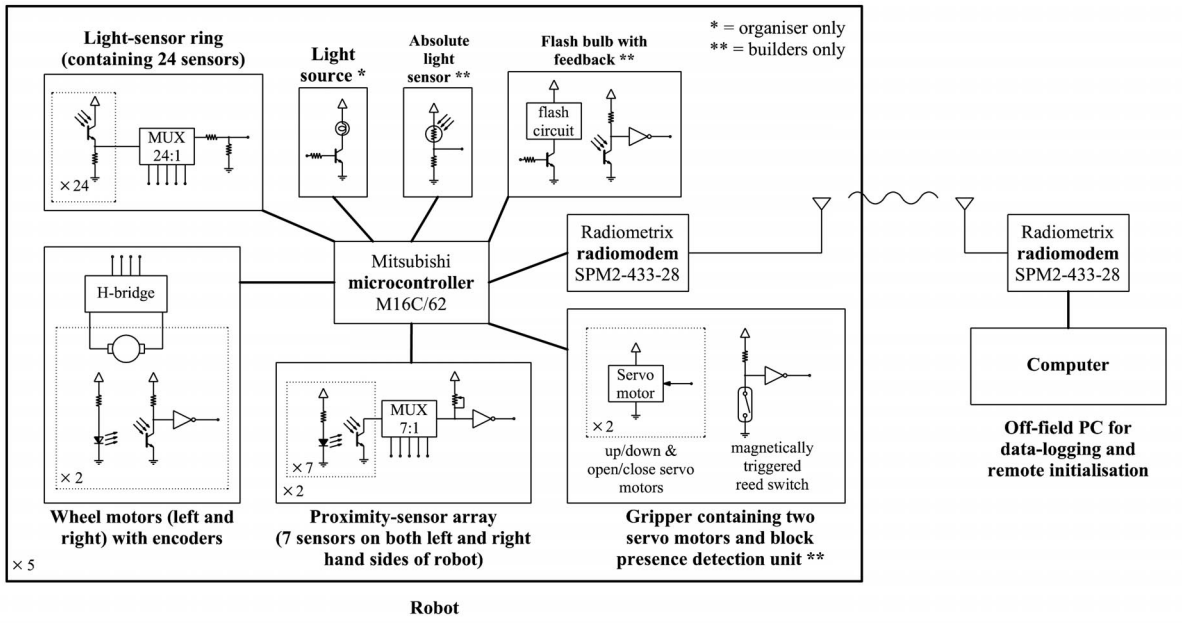

Figure 2. This figure shows the different subsystems that make up a robot, each of which is interfaced to a central microcontroller. Each subsystem is powered from a 5 V regulated supply drawn from a 12 V battery (not shown). Radiomodems facilitate communication to and from an off-field computer, allowing robot initialisation and data logging. A more thorough description of the hardware and software is provided in [5].

the popular subsumption architecture [27].

Rule Set 1 Organiser robot rule set.

1: **If** number of deposition windows completed equals the total number of deposition windows required **Then** turn off light bulb
2: **If** *flash_count_max* flashes have been detected for the current deposition window or the trial has just been started **Then** move/rotate a distance given by the next value in the sequence b_n and change the light source voltage to the next value from the sequence a_n
3: Count flash signals

In the following sections, simulation and mathematical models are introduced for the purpose of gaining additional insight and understanding into the deposition process and feedback system. The models capture the dynamics observed during practical trials, explaining why the rate of deposits decreases and frustration levels increase, on average, with each new deposit attempt made. These dynamics play an important role in the operation of the feedback system. The models also predict the occurrence of patterns of blocks within deposition windows, and help to explain why such a phenomenon occurs. Each model is based on the behaviour of the real robots and geometrical constraints of the hardware.

3. Simulation model

3.1. Formulation of the simulation model

As previously mentioned, the organiser robot carries a light source which emits light in a beam of $\theta = 30\,^\circ$. The light beam is depicted in Figure 4 with a builder robot also shown, located in the light field gradient at

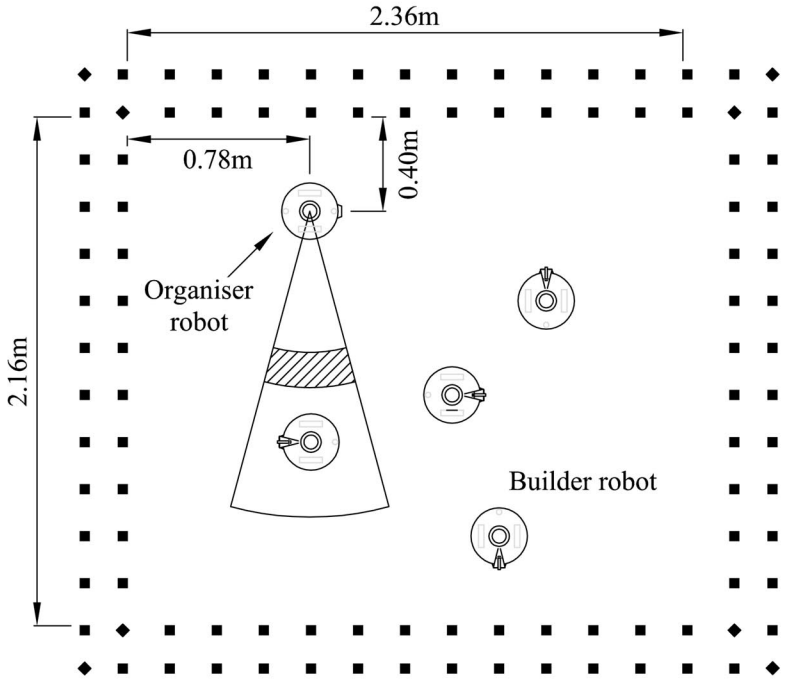

Figure 3. The experimental set-up from [5] showing the initial configuration of robots and building blocks. The organiser robot's light-beam template is depicted, with hatching used to indicate the deposition window.

the coordinates (r_0, α_0). In the beam, the light intensity is a monotonically decreasing function of distance (r) from the light source[3]. Builder robots are programmed to deposit within a fixed window of intensity corresponding to the spatial region, $r_1 \leq r \leq r_2$, called the deposition window.

A simulation run is defined as a number of deposit attempts by one or more builder robots. A deposit attempt begins when a builder robot, that is carrying a building block, recognises that it is inside the beam and starts to drive up it (along a radial line) towards the light source (rule 6, Rule Set 2). It will be said that a deposit attempt ends in either success (where a block is deposited) or failure (where the builder robot is unable to move into the deposition window). It is assumed that a failed attempt to deposit is the result of one or more blocks inhibiting access to the deposition window. Scenarios where other robots cause deposit attempt failures by getting in the way are not considered.

The spatial location of the point at which a robot begins driving up the beam is denoted by (α_0, r_0) in Figure 4. In practice, the location of this point is thought to be dependent on a number of interrelated factors. These factors include the (i) number and location of robots inside the beam, (ii) obstacle avoidance behaviour, (iii) behaviour after failing to deposit, (iv) beam length and, (iv) behaviour on first detecting the beam. For the purposes of simplicity however, we assume the location of this point to be uniformly distributed within the limits $0 \leq \alpha_0 \leq \theta$ and $r_2 + R + \eta \leq r_0 \leq r_3$ (where R and η are defined later and

[3]Here we assume the light source is an ideal point source and the absolute light sensor is an ideal point receptor. In practice, the size, and variations in the orientation and inclination of the source and receptor may cause the detected light intensity to depart from being a monotonically decreasing function of distance. Furthermore, environmental noise can influence the light intensity that is detected by a robot. For simplicity these factors have not been modelled in this study, although it may be useful to consider their inclusion in future work (see Section 4.3.2).

Rule Set 2 Builder robot rule set.

1: **If** not holding block and not in beam and object detected **Then** attempt to pick up object
2: **If** holding block and in deposition window **Then** deposit block behind another block or at inner window limit and reset frustration counter
3: **If** holding block and have just arrived in beam **Then** drive further into beam avoiding obstacles if detected
4: **If** frustration counter equals 2 **Then** flash light and reset frustration counter
5: **If** holding block and in beam and obstacle detected **Then** increment frustration counter, turn randomly $\pm 135^\circ$ and then drive forwards
6: **If** holding block and in beam **Then** drive up beam towards light
7: **If** obstacle detected **Then** avoid obstacle
8: Drive forwards

in Figure 5). That is, the starting point of each approach is independent of previous approaches. Practical results suggest that the assumption is broadly valid (see [5, Section 6.2.1]).

The behaviour of a simulated builder robot replicates the behaviour of a real builder robot. When driving up the beam, a builder robot will make periodic stops (separated by a distance, g) during which it checks whether or not it is in the deposition window (see Figure 4). Once the robot recognises that it is inside the deposition window it continues to move towards the light source until it crosses over the inner window limit or detects another block (rule 2, Rule Set 2). At this point, it reverses and deposits the block that it is currently holding. Figure 5 shows that the deposited block placement is offset a distance, d, from the centre position of the robot before it started to reverse. This distance is a consequence of trying to place blocks close to one another [5, Section C.4.3].

In practice, blocks are detected by a real robot's array of IR proximity sensors. This is modeled as a region where objects are detected and is represented by an annular arc of 180° and width, η (Figure 5). The smallest distance that the simulated robot is able to move is ζ. As a consequence, this means that the robot cannot stop immediately on detecting an object. Instead, objects are detected within a distance $[R+\eta-\zeta, R+\eta]$ from the centre of the robot, where R is the radius of the robot.

The simulation model introduced in this section was programmed in C/C++ and compiled under Windows. To provide user feedback, a graphical display was implemented using the Qt class library. Data from each simulation run was saved in an output file. A MATLAB script then used the data files to generate plots of the results. Based on measurements obtained from the real robots, the following parameter values were used in the simulation and throughout this paper: $g = 21.8$ mm, $d = 39.2$ mm, $\eta = 16.5$ mm, $\zeta = g/2 = 10.9$ mm and $R = 0.12$ m.

3.2. Simulation results

3.2.1. Deposition window block configurations

The configuration of blocks within a deposition window is highly variable. Figure 6 shows a number of results from typical simulation runs with the number of deposit attempts $= 20$. Values of $r_1 = 0.6$ m, $r_2 = 0.75$ m, $r_3 = 1.3$ m were chosen and are used throughout this paper, except where otherwise stated. The results indicate that some block configurations are more compact than others, with differing numbers of blocks deposited in each deposition window. This effect becomes more noticeable for relatively large deposition windows where large internal cavities can arise. For example, in Figure 7 an atypically large deposition window is shown. In it, blocks have been labelled to indicate the order in which they were deposited and arrows have also been added to indicate when one block caused another block to be deposited. A stigmergic

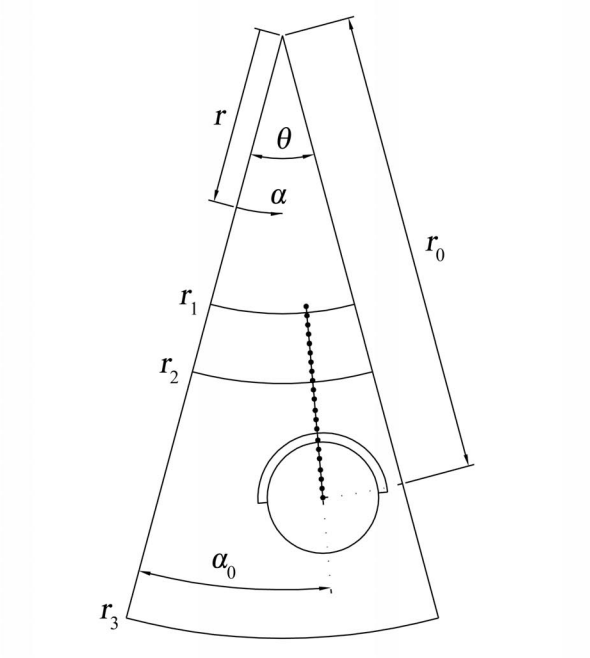

Figure 4. A builder robot located at an initial position of (α_0, r_0). Its path towards the light source consists of discrete stops (separation, g), marked as small filled circles, at which the light level is sensed. Once inside the deposition window ($r_1 \leq r \leq r_2$) the robot will inevitably deposit a block.

process (under the control of the template) can clearly be seen where previously deposited blocks trigger other blocks to be deposited. In this example, block 4 triggered block 5 to be deposited, which triggered block 7 to be deposited and so on. As a consequence of this stigmergic action and, as a result of choosing a random approach angle, blocks are not always placed as compactly as they could be.

The block configurations observed in practical trials form similar patterns to those obtained in simulation. Consider Figure 8(a) which shows a loose linear wall being constructed by a swarm in an experimental trial (viz. Trial 14 reported in [24]). During this trial an organiser robot was programmed with a recipe to move and make stops along a straight line, creating a spatio-temporal varying template with its light source. Through this process, five adjacent deposition windows were sequentially created by the organiser robot and filled with blocks by builder robots. The blocks associated with each deposition window are highlighted in Figure 8(b).

It should be noted that Trial 14 in [24] is used as an example throughout this paper as in this particular trial there were relatively few atypical happenings. Also, the value of *flash_count_max* used (in Rule Set 1) was relatively high, meaning more deposit attempts would have been made per window and, as a result, trends from the data are better observed.

From the practical results it can be seen that, as in simulation, the number of blocks in each deposition window varies and is related to the compactness of the deposited blocks. This compactness is, in turn, related to the sequence of approach angles chosen that lead to deposits. For a compact structure, the deposition window tends to grow outwards evenly. On the other hand, less compact structures arise when consecutive approach angles are similar. This leads to non-uniformity of growth which, for large windows, can result in internal cavities (as is seen in Figure 7). Deposition windows of smaller depth can be more compact, since

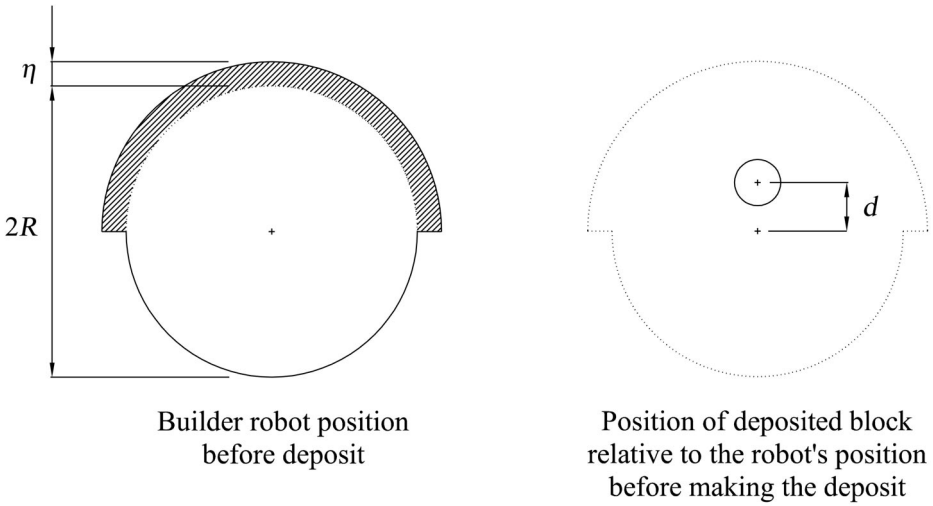

Figure 5. (a) The model of a builder robot with key dimensions highlighted. (b) The relative placement of a deposited block. The shaded annular strip represents the area where objects are detected by the array of IR proximity sensors. Note that the absolute light sensor is located at the centre of the robot.

outwards growth is forced to be uniform. In the limit, when the deposition window depth is sufficiently small, so that only a single layer of blocks can be deposited, the stigmergic action is reduced or non existent, and there is no scope for internal cavities to arise within an individual deposition window.

3.2.2. Success and failure in deposit attempts

In addition to the graphical results obtained from the simulations, interesting quantitative data was also collected. Simulation runs were conducted in which a fixed number of deposit attempts were made (viz. 20). The outcome of each attempt was recorded as either a success or a failure. A total of 200 simulation runs were performed, and the results averaged. Figure 9 shows the average number of successes and failures versus the number of deposit attempts. It can be seen that as the number of attempts made increases, the number of blocks in the deposition window (equivalent to the number of successes) increases linearly at first before heading towards a horizontal asymptote. This is in contrast to the average number of failed attempts which is zero for some time and then slowly begins to increase before rising indefinitely towards a slant asymptote. (Note, the number of failures + number of successes = number of attempts.)

Intuitively the results make sense. When the deposition window is empty, blocks are successfully deposited. However, as it begins to fill, robots start to become frustrated (through attempt failures). At some point, determined by the size of the deposition window, there is little gain to be had in making further deposit attempts. This finding is consistent with the practical results obtained in [24].

It is also informative to look at the result for a single run of the simulation. Figure 10 shows the number of successful and failed deposit attempts for a particular trial. Since the outcome of a deposit attempt is discrete, the points used to construct each curve occur at integer coordinates. The simulation

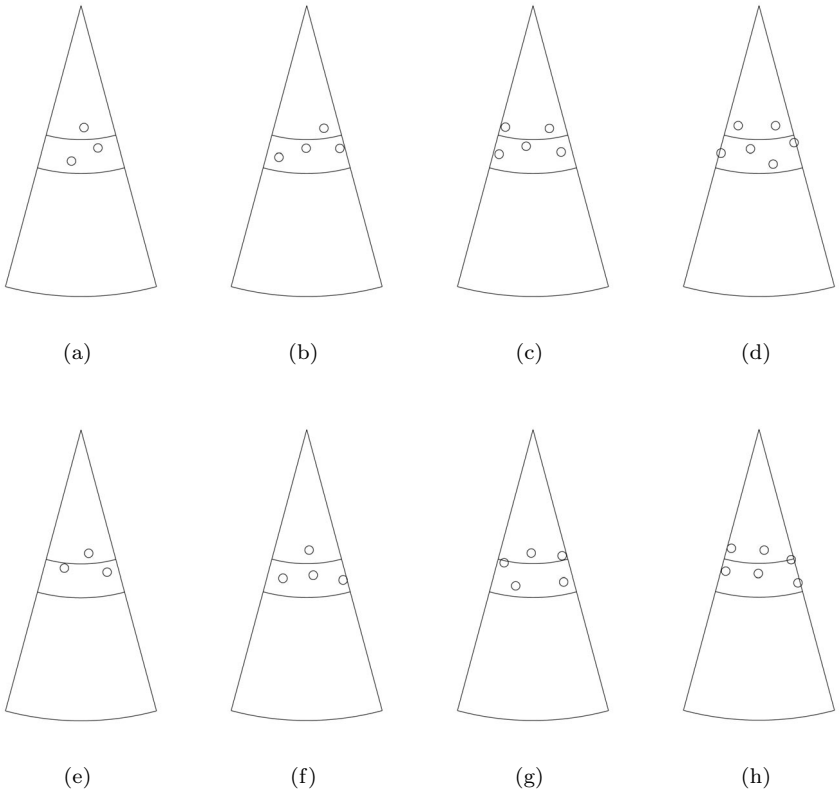

Figure 6. A selection of different block configurations obtained in simulation runs with the number of deposit attempts = 20.

results are similar to the results obtained in practical trials. For example, Figures 11 and 12 show the success and failure curves for the first deposition window of Trial 14 in [24]. The curves are mostly within ± 2 standard deviations of the simulation mean. Also, the trends are similar in shape to the simulation trends and the asymptote values are of the correct order of magnitude. This suggests that the simulation model may contain sufficient detail to be useful as a tool for quantitative prediction. However, it is felt that many more experimental trials would be necessary to fully validate this.

The simulation model presented has produced results that are consistent with the results from practical robot trials. Specifically, the patterns of blocks generated in deposition windows are similar to those observed in practical trials. Variability in the number of blocks deposited in a window is also explained through the simulation. Trends, that predict how the number of successful and failed deposits increases with the number of attempts made, also conform to observations made in practical trials. While the simulation model is sufficient to make predictions about the practical deposition process, further insight can be gained through the development of a mathematical model and this is the subject of the next section.

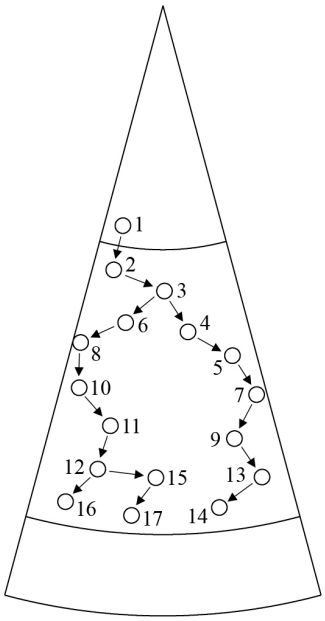

Figure 7. Block placements for an atypically large window size obtained from a simulation with $r_1 = 0.6$ m, $r_2 = 1.3$ m, $r_3 = 1.5$ m and number of deposit attempts = 100. Blocks are labelled according to the order in which they were deposited. Arrows are used to indicate when a block caused another to be deposited (under the guidance of the template).

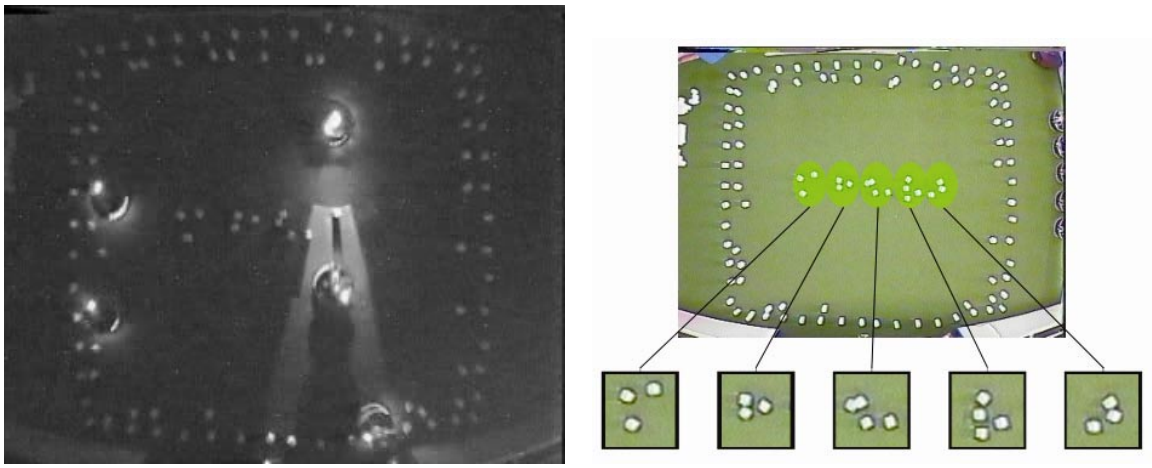

(a) (b)

Figure 8. Images of the test area (a) during and (b) after the completion of Trial 14 in [24]. In this trial, a loose linear wall structure was built by builder robots using blocks collected from the periphery of the test area (see Figure 3). In (a) the fourth deposition window can be seen in the process of being filled. The organiser robot's light beam is clearly evident with a builder robot approaching towards the construction zone. The block configuration in each of the five deposition windows used has been highlighted in (b), where the robots have been removed for clarity.

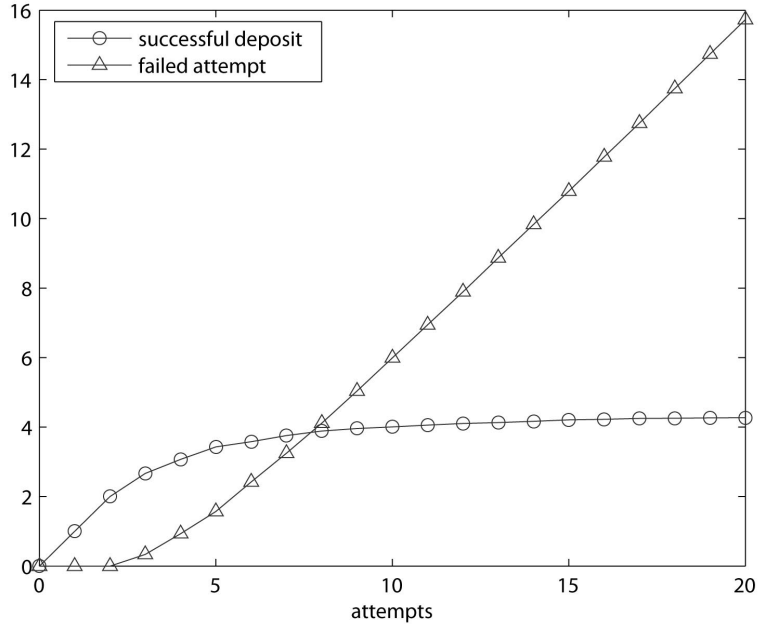

Figure 9. The average number of successes and failures versus the number of deposit attempts. Results obtained from the average of 200 simulation runs.

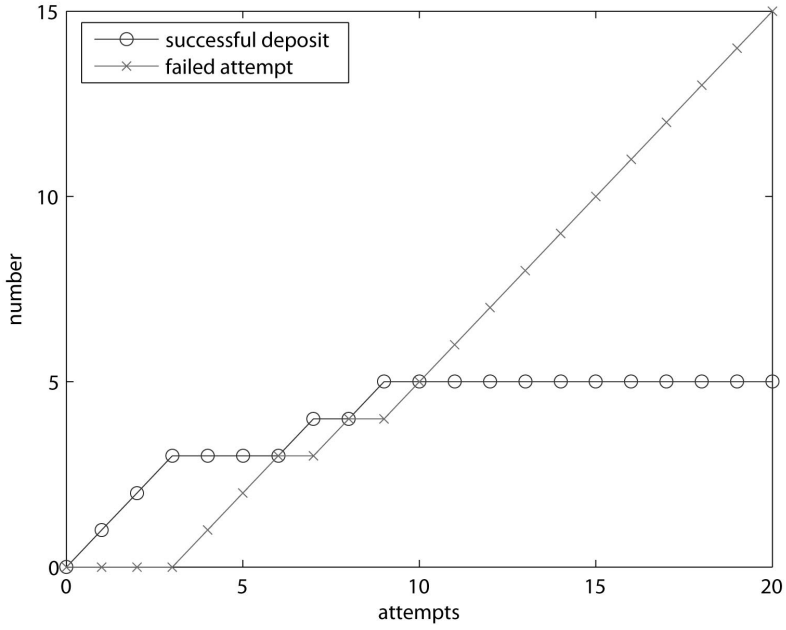

Figure 10. The results for a single typical simulation run showing the number of successes and failures versus the number of deposit attempts.

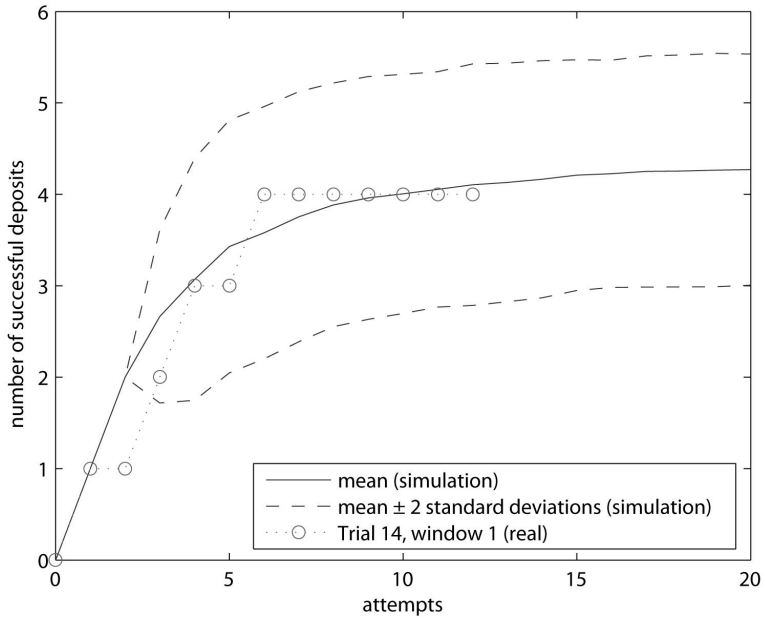

Figure 11. The number of successful deposits versus the number of deposit attempts made. Simulation results (mean ± 2 standard deviations) as well as a practical result (first deposition window, Trial 14 in [24]) are shown. Simulation results were obtained from the data for 200 simulation runs.

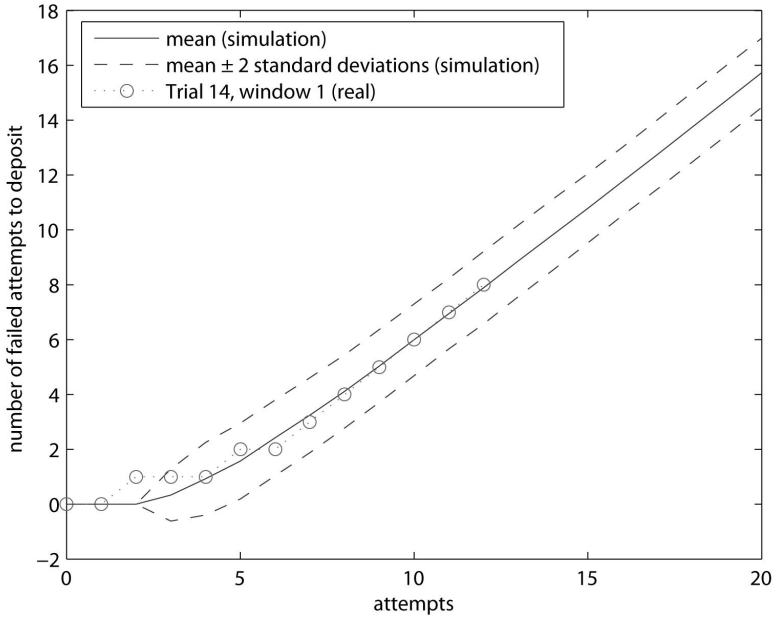

Figure 12. The number of failed attempts to deposit versus the number of deposit attempts made. Simulation results (mean ± 2 standard deviations) as well as a practical result (first deposition window, Trial 14 in [24]) are shown. Simulation results were obtained from the data for 200 simulation runs.

4. Mathematical Model

In this section a mathematical model for the deposition process is detailed. In the derivation that follows, a number of simplifying assumptions will be made. This is done in order to allow for the development of an analytical model. However, because of the assumptions made, the ability of the model to make accurate quantitative predictions is reduced. Nevertheless, the analytical model brings considerable insight into the processes at work in the system and also allows predictions to be made.

4.1. Approximating compact block placement with a lattice structure

As has been noted, the placement of blocks within the deposition window is different for each trial. It would seem however, that there could be some optimal packing arrangement that, given favourable circumstances, might arise. Consider the hexagonal lattice structure, shown in Figure 13. The structure is composed of disks arranged in horizontal layers. This hexagonal arrangement is known to be compactly optimal in terms of the number of disks per unit area [28]. The distance between adjacent disk centres is Δ and horizontal layers are separated by a distance of $c = (\sqrt{3}/2) \cdot \Delta$. Each disk represents a location that holds a block. Each block is approximated as a circle of radius, B, where $B \leq \Delta$.

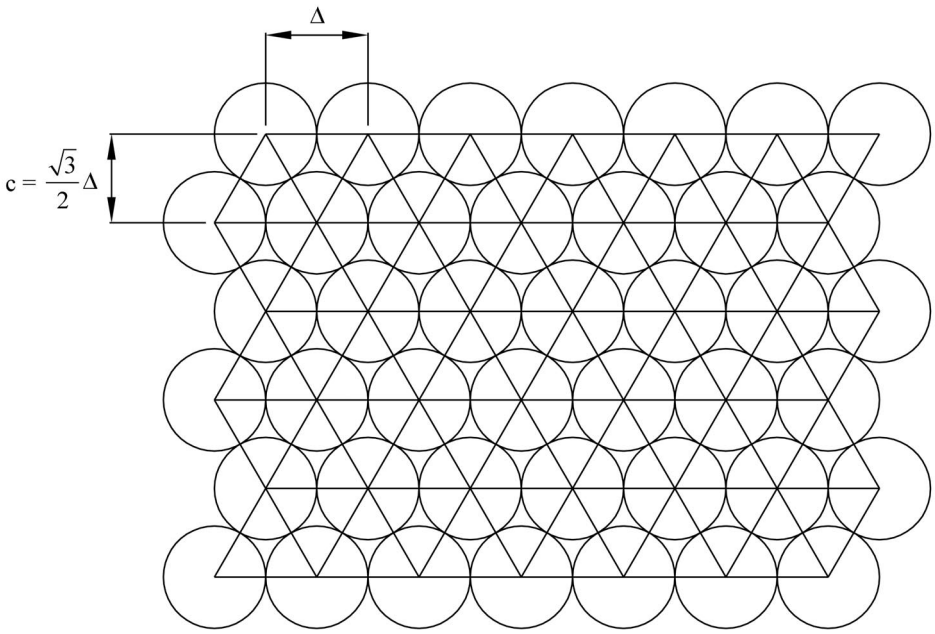

Figure 13. A conceptual lattice structure composed of disks separated by Δ, and layers separated by $c = (\sqrt{3}/2) \cdot \Delta$. Each disk represents a potential location for a block and is regarded as either filled or empty.

Figure 14 shows a deposition window (approximated as a quadrilateral) that has been filled with a hexagonal lattice structure containing a fixed number of disks. In general, it will be said that a lattice structure is composed of z layers, each of which contains m_k disks (where k is the layer number). The

number of layers in the lattice structure is given by:

$$z = \text{truncate}\left(\frac{r_2 - r_1}{c}\right) + 1 \tag{1}$$

After determining geometrically how many disks can be placed adjacent in a straight line of fixed length, the following expression is given for the number of disks in the k^{th} layer:

$$m_k = \text{truncate}\left(\frac{2(r_1 - d + (k-1)c)\sin\frac{\theta}{2}}{\Delta}\right) + 1 \tag{2}$$

$$k \in \{1, 2, \ldots, z\}$$

These expressions were chosen as a coarse approximation to how a lattice structure might be fitted into a given deposition window.

It has been stated that each disk represents a location for a block, but what should the radius, Δ, of the disks be? Limitations posed by the robot's behavioural algorithms and robotic hardware prevent the most compact arrangement of blocks ($\Delta = 2B$) from ever occurring. On some occasions blocks will be placed close together, on other occasions, further apart. Compensating for this effect means choosing an appropriate value for Δ. One possible choice for Δ could be the average value, $\bar{\delta}$, of the distance between the centres of stigmergically linked blocks[4].

When a builder robot detects a block inside the deposition window, it deposits the block that it is currently carrying. The distance, δ, between the centres of the newly deposited and previously deposited blocks, depends on a number of factors. These include (i) the location of the previously deposited block, (ii) the approach angle of the robot (α_0) and, (iii) where within the object detection region the block is first detected. An analytic expression will now be derived to determine a general expression for the distance between stigmergically linked blocks (δ), and from this, an expression for $\bar{\delta}$ ($= \Delta$) follows.

4.2. Determining the average distance between stigmergically linked blocks

To begin with, let us consider a situation where a robot is located at some position, P_0, at time, t_0. This is depicted in Figure 15 where a coordinate system has been established with respect to some previously deposited block (whose centre is located at the origin). The block is at a distance, r_B, and angle, α_B, with respect to the light source, and it has a radius, B. The distance between centres of the robot and the block is denoted by ε. At time t_1, the robot moves forward a distance, ζ, along its trajectory towards the light source. At its new location, P_1, it will be said that it detects the previously deposited block. The distance, between the centres of the robot's new position and the block is:

$$D = \sqrt{\varepsilon^2 + \zeta^2 - 2\varepsilon\zeta\sqrt{1 - \left(\frac{r_B}{\varepsilon}\sin\varphi\right)^2}} \tag{3}$$

By considering the extreme cases, limits for the variable ε can be assigned. Firstly, the lower limit on ε is determined by considering the situation where the block is just out of detection range when the robot

[4]The phrase stigmergically linked is used to describe blocks that have been deposited as a result of other blocks being detected. That is, two blocks are stigmergically linked when one has caused another to be deposited (under the guidance of a template). For example, arrows were used in Figure 7 to show stigmergically linked blocks.

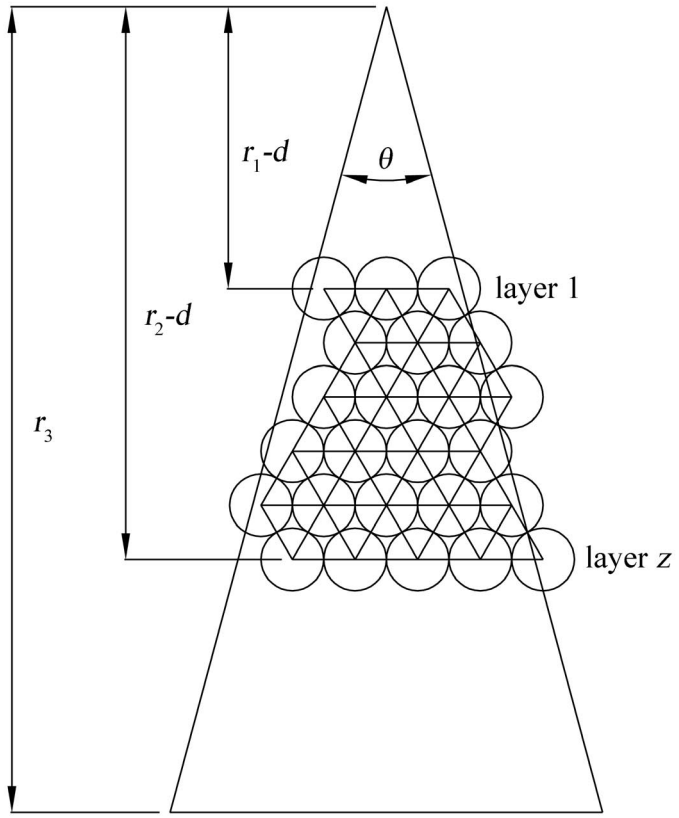

Figure 14. Lattice structure chosen to fill a deposition window (approximated as a quadrilateral).

is located at P_0. Secondly, the upper limit on ε is determined by considering the situation where the block is just being detected when it is located at P_1. Based on these two extreme cases, it can be found that ε must lie within the range:

$$\begin{aligned} R+\eta+B &\leq \varepsilon \\ &\leq \sqrt{(R+\eta+B)^2+\zeta^2+2(R+\eta+B)\zeta\sqrt{1-\left(\tfrac{r_B}{R+\eta+B}\sin\varphi\right)^2}} \end{aligned} \tag{4}$$

In the analysis that follows, it is assumed that ε is uniformly distributed in the range given by Eq. (4).

With reference to Figure 15, the builder robot's coordinates, $(x_{robot}, -y_{robot})$, can be defined with reference to the parametric equations:

$$x_{robot} = D\sin\left(\varphi+\sin^{-1}\left(\frac{r_B\sin\varphi}{D}\right)\right) \tag{5}$$

$$y_{robot} = D\cos\left(\varphi+\sin^{-1}\left(\frac{r_B\sin\varphi}{D}\right)\right) \tag{6}$$

where $0 \leq \varphi \leq \sin^{-1}\left(\frac{R+\eta+B}{r_B}\right)$ and $\varphi = \alpha_0 - \alpha_B$.

Note that here only the situations where a robot detects a block to its left will be considered. Situations where the block is to the right of the robot would follow a similar analysis.

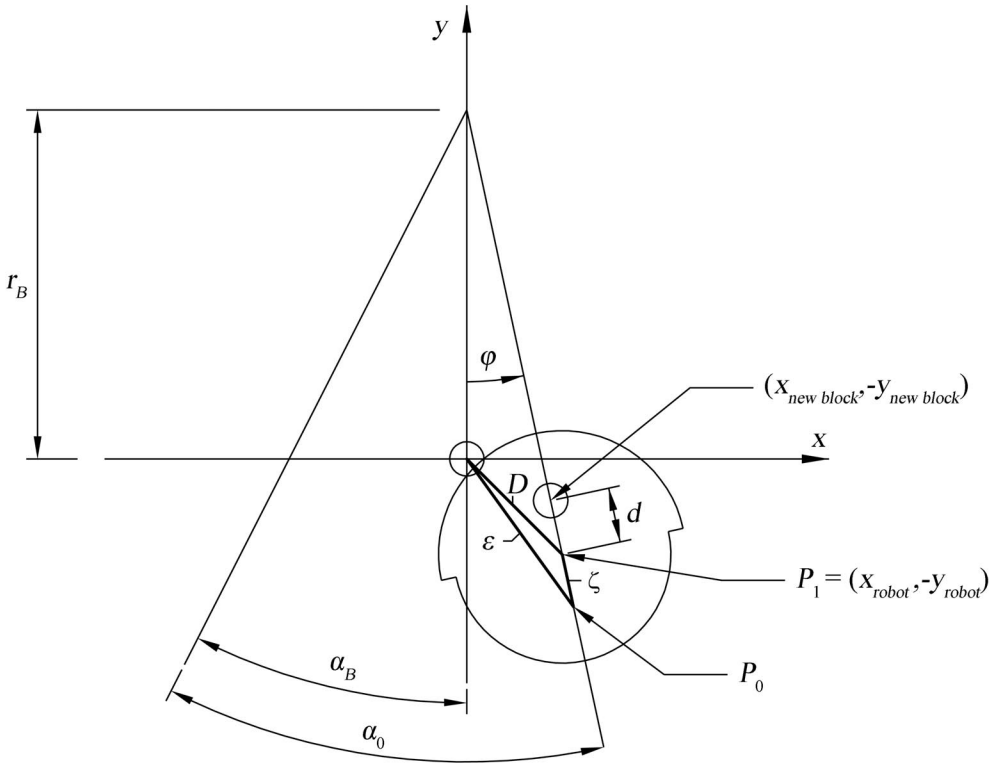

Figure 15. A new coordinate system established with respect to a previously deposited block (located at the origin). The light source is located at $(0, r_B)$. A builder robot is shown at P_1 detecting the previously deposited block. Prior to this, the builder robot was located at P_0 where the block was not able to be detected. Having detected the block, the robot then moves and deposits a new block at the coordinates $(x_{new\ block}, -y_{new\ block})$.

When the previously deposited block is detected, the robot reverses back along its radial approach line and makes a deposit. The location of the newly deposited block is given by the coordinates $(x_{new\ block}, -y_{new\ block})$, which can be defined with reference to the following parametric equations:

$$x_{new\ block} = x_{robot} - d\sin\varphi \tag{7}$$

$$y_{new\ block} = y_{robot} - d\cos\varphi \tag{8}$$

where φ is defined as before, viz.: $0 \leq \varphi \leq \sin^{-1}\left(\frac{D}{r_B}\right)$.

An expression for the distance between centres of the previously deposited block and the newly deposited block can now be formulated. Equation (9) gives this distance, δ, which is a function of φ, r_B

and ε.

$$\begin{aligned}\delta(r_B,\varphi,\varepsilon) &= \sqrt{x^2_{new\ block}+y^2_{new\ block}} \\ &= \sqrt{D^2+d^2-2dD\sin\left(2\varphi+\sin^{-1}\left(\frac{r_B\sin\varphi}{D}\right)\right)}\end{aligned} \tag{9}$$

where D, a function of ε, is given by Eq. (3).

Equation (10) gives the average [29] distance between the centres of a previously deposited block and a newly deposited block. This distance, $\bar{\delta}$, will be called the average distance between stigmergically linked blocks. It is obtained by integrating Eq. (9) over the range of possible φ, r_B and ε values and this is readily done using numeric integration.

$$\overline{\delta} = \frac{\int_{r_1}^{r_2}\int_{\varphi_1}^{\varphi_2}\int_{\varepsilon_1}^{\varepsilon_2}\delta(r_B,\varphi,\varepsilon)\,\mathrm{d}\varepsilon\,\mathrm{d}\varphi\,\mathrm{d}r_B}{\int_{r_1}^{r_2}\int_{\varphi_1}^{\varphi_2}\int_{\varepsilon_1}^{\varepsilon_2}1\,\mathrm{d}\varepsilon\,\mathrm{d}\varphi\,\mathrm{d}r_B} \tag{10}$$

where $\delta(r_B,\varphi,\varepsilon)$ is given by Eq. (9).

As stated, the integration in Eq. (10) is performed over the range of possible values for r_B, φ, and ε. Specifically, r_1 and r_2 define the deposition window and φ_1, φ_2, ε_1 and ε_2 are simply the limits placed on φ and ε which were determined earlier. In other words,

$$\varphi_1 = 0, \tag{11}$$

$$\varphi_2 = \sin^{-1}\left(\frac{R+\eta+B}{r_B}\right), \tag{12}$$

$$\varepsilon_1 = R+\eta+B, \tag{13}$$

and

$$\varepsilon_2 = \sqrt{(R+\eta+B)^2+\zeta^2+2(R+\eta+B)\zeta\sqrt{1-\left(\frac{r_B}{R+\eta+B}\sin\varphi\right)^2}}. \tag{14}$$

By modelling block separation in terms of one parameter, $\bar{\delta}$, an attempt is being made to discretise what is an inherently continuous process; where block placement is variable and separation between blocks is also variable. It should be noted that Eq. (10) is an approximation because the integration limits allow some combinations of the three variables $(\varepsilon,\varphi,r_B)$ that violate $0\le\alpha_0\le\theta$ (see [5, Section 6.3.2] for further details).

It has now been shown that by considering the deposition behaviour and hardware constraints of the robots, an average distance of separation between the centres of two stigmergically linked blocks can be found (i.e. $\bar{\delta}$). Using this result, it is now possible to continue with the formulation of the lattice structure model by letting $\Delta=\bar{\delta}$.

4.3. Modelling the deposition process with a Markov chain

Thus far, it has been considered that each disk in the lattice represents the location for a block separated from neighbouring blocks by a distance, $\Delta = \bar{\delta}$. In practice however, there is nothing to force blocks to be deposited in a compact structure similar to that of the lattice model. Often previously deposited blocks will inhibit robots from getting as close as they possibly could to the inner deposition window limit. This gives rise to gaps in the deposition window as was evident in Figures 6 and 7. In terms of the lattice model, this is equivalent to gaps arising when blocks are deposited in the outer layers before the inner layers are complete. Probabilistically speaking, as the outer layers begin to fill, the chance of an inner layer being completed reduces, since the outer layer blocks prevent access to the inner layers. This effect can be added to the formative model simply by assigning probabilities that disks in the lattice will attain a block[5].

Starting with an empty deposition window, it is considered that a trial consists of a number of deposit attempts, N_A. Here, a trial is analogous to a simulation run. Each deposit attempt may either succeed or fail. Success means that a block is successfully deposited. Failure means that a robot does not deposit because it is unable to get into the deposition window (due to previously deposited blocks getting in the way).

The state of the deposition window, after some arbitrary number of deposit attempts, is defined by the vector, Eq. (15). This state vector takes account of the number of blocks occupying the disks in each layer. Note that for simplicity, different combinations of block positions within each layer, are not considered in this model.

$$\mathbf{s}_i = \begin{bmatrix} s_{i,1} \\ s_{i,2} \\ \vdots \\ s_{i,z} \end{bmatrix} \tag{15}$$

where $s_{i,k}$ is the number of blocks in the k^{th} layer and $k \in \{1, 2, \ldots, z\}$. Here, z is given by Eq. (1).

When another deposit attempt is made, the state, $\mathbf{s}_i$, transitions to itself or to one of z other states. That is, $\mathbf{s}_i \rightarrow \mathbf{s}_{ij}$ where $j \in \{i, 1, 2, \ldots, z\}$. These new states are given by the column vectors of Eq. (16).

$$\begin{aligned} &\begin{bmatrix} \mathbf{s}_{ii} & \mathbf{s}_{i1} & \mathbf{s}_{i2} & \cdots & \mathbf{s}_{iz} \end{bmatrix} \\ &\quad = \begin{bmatrix} \mathbf{s}_{ii} & \begin{bmatrix} \mathbf{s}_i & \mathbf{s}_i & \cdots & \mathbf{s}_i \end{bmatrix} + \mathbf{I} \end{bmatrix} \\ &\quad = \begin{bmatrix} s_{i,1} & s_{i,1}+1 & s_{i,1} & \cdots & s_{i,1} \\ s_{i,2} & s_{i,2} & s_{i,2}+1 & \cdots & s_{i,2} \\ \vdots & \vdots & \vdots & \ddots & \vdots \\ s_{i,z} & s_{i,z} & s_{i,z} & \cdots & s_{i,z}+1 \end{bmatrix} \end{aligned} \tag{16}$$

where $\mathbf{I}$ is a $z \times z$ identity matrix. Note that $\mathbf{s}_{ii} \equiv \mathbf{s}_i$.

The probability that the state, $\mathbf{s}_i$, transitions to some state, $\mathbf{s}_{ij}$, is given by q_{ij}. The vector, $\mathbf{q}$,

[5]Note that we are now at a level of abstraction where the robot can be considered as a point.

defined in Eq. (17), contains all of the transition probabilities from q_{ii} to q_{iz}.

$$\mathbf{q} = \begin{bmatrix} q_{ii} \\ q_{i1} \\ q_{i2} \\ \vdots \\ q_{iz} \end{bmatrix} \tag{17}$$

where it is noted that the element, q_{ii}, which defines the probability that $\mathbf{s}_i$ transitions to itself, is included in the vector matrix.

In formulating actual expressions for the transition probabilities given in Eq. (17), it is necessary to consider the deposition behaviour of the robots. When a robot is approaching the light source along a radial line, it attempts to enter the deposition window. The chance that it is able to do this successfully will depend on the likelihood that there isn't a block in its path. In terms of the lattice model, if the outermost (last) layer (z) is close to being full, the chance of failure is high. Failure means that the robot's frustration counter is incremented (rule 5, Rule Set 2). On the other hand, if the outermost layer is empty, then a deposit will definitely be made somewhere within the deposition window.

The probability that the deposition window is not entered successfully is assumed to be the probability that a block is detected in the outermost layer. This can be equated to the ratio of the number of filled disks in the outermost layer to the total number of disks in that outermost layer (m_z, defined in Eq. (2)). It is equal to the probability, q_{ii}, that the process stays in the same state, $\mathbf{s}_i = \mathbf{s}_{ii}$. That is,

$$\Pr(\text{failure to deposit}) = \frac{s_{i,z}}{m_z} = s_{i,z} g_z \tag{18}$$

where g_z forms part of the vector, $\mathbf{G}$, defined as:

$$\mathbf{G} = \begin{bmatrix} 1/m_1 \\ 1/m_2 \\ \vdots \\ 1/m_z \end{bmatrix} = \begin{bmatrix} g_1 \\ g_2 \\ \vdots \\ g_z \end{bmatrix} \tag{19}$$

On successfully entering the deposition window, a robot will continue to move along a radial path towards the light source. As soon as it crosses the inner deposition window limit or encounters a previously deposited block, it will make a deposit. The chance of it reaching the inner deposition window limit without encountering a block on the way depends on the number of blocks already deposited and the layers in which they are located. The closer previously deposited blocks are to the inner window limit, the further the robot will be able to travel towards the light source before making a deposit. In terms of the lattice structure model, this can be thought of as journeying towards the inner window limit whilst passing through different layers on the way. The chance of passing successfully through some layer without being forced to make a deposit is equivalent to not encountering a block in that layer. The probability of this happening is defined as:

$$\begin{aligned} & \Pr(\text{passing through layer } k) \\ = \; & \Pr(\text{not depositing a block in layer } k \mid \text{trying to deposit in layer } k) \\ = \; & 1 - s_{i,k} g_k \end{aligned} \tag{20}$$

where $k \in \{2, 3, \ldots, z\}$.

From this, it is clear that if the robot is trying to pass through a layer that is full, then the chance that it will do so successfully, is zero. On occasions such as these, the robot will be forced to make a deposit in the current layer or, if outside the deposition window, it will fail in its attempt to make the deposit.

Once the inner deposition window limit has been reached, a robot will always make a deposit. That is to say, it is not possible to pass through layer 1:

$$\Pr(\text{passing through layer 1}) = 0$$

Using Eq. (20) and based on the state of the deposition window, $\mathbf{s}_i$, it is now possible to write down expressions for the transition probabilities given in Eq. (17). The vector $\mathbf{q}$ is fully defined as:

$$\mathbf{q} = \begin{bmatrix} q_{ii} \\ q_{i1} \\ q_{i2} \\ \vdots \\ q_{iz} \end{bmatrix} = \begin{bmatrix} s_{i,z} g_z \\ (1) \cdot \prod_{k=1}^{z} (1 - s_{i,k} g_k) \\ (s_{i,1} g_1) \cdot \prod_{k=2}^{z} (1 - s_{i,k} g_k) \\ \vdots \\ (s_{i,z-1} g_{z-1}) \cdot \prod_{k=z}^{z} (1 - s_{i,k} g_k) \end{bmatrix} \tag{21}$$

We have now arrived at a point where, given some known lattice configuration ($\mathbf{G}$) and a state for the deposition window ($\mathbf{s}_i$), it is possible to generate a list of possible new states $\{\mathbf{s}_{ii}, \mathbf{s}_{i1}, \mathbf{s}_{i2}, \ldots, \mathbf{s}_{iz}\}$ and their associated transition probabilities ($\mathbf{q}$). From the valid new states (that is, states with all input transition probabilities being nonzero), further new states can be generated in a similar manner. In this way, by repeated application of Eq. (16) and Eq. (21) it is possible to generate a finite length Markov chain with all possible valid states and their transition probabilities fully defined.

The Markov chain is finite because there is a certain limit, N_{states}, to the maximum number of different block configurations allowed within the deposition window, and the number of allowed states, $N_{allowed}$, cannot exceed this upper bound. That is, $N_{allowed} \leq N_{states}$. Here, $N_{allowed}$ is determined by counting the number of states after the Markov chain has been formulated, and the upper bound, N_{states}, is given by:

$$N_{states} = (m_1 + 1) \times (m_2 + 1) \times \ldots \times (m_z + 1) \tag{22}$$

As an example, consider a lattice structure with $z = 2$, $m_1 = 2$ and $m_2 = 2$. Using Eq. (22), the maximum number of states is $N_{states} = 9$. These states are: $[\ 0 \quad 0\ ]^T$, $[\ 0 \quad 1\ ]^T$, $[\ 1 \quad 0\ ]^T$, $[\ 1 \quad 1\ ]^T$, $[\ 1 \quad 2\ ]^T$, $[\ 2 \quad 1\ ]^T$, $[\ 2 \quad 2\ ]^T$, $[\ 2 \quad 0\ ]^T$ and $[\ 0 \quad 2\ ]^T$. However, by formulating a Markov chain for this example, it is found that $N_{allowed} = 7$ and the states, $[\ 0 \quad 1\ ]^T$ and $[\ 0 \quad 2\ ]^T$, are invalid.

All Markov chains constructed using the above procedure are found to have both transient and absorbing states. Using standard Markov chain analysis techniques, the probability of being in each state after a given number of deposit attempts can be calculated. Before doing this, each state is uniquely labelled $\{\mathbf{A}_1, \mathbf{A}_2, \ldots, \mathbf{A}_{allowed}\}$ and the transition probabilities between all states are also labelled and expressed in

matrix form:

$$\mathbf{P} = \begin{bmatrix} p_{11} & p_{12} & \cdots & p_{1N_{allowed}} \\ p_{21} & p_{22} & \cdots & p_{2N_{allowed}} \\ \vdots & \vdots & \ddots & \vdots \\ p_{N_{allowed}1} & p_{N_{allowed}2} & \cdots & p_{N_{allowed}N_{allowed}} \end{bmatrix} \tag{23}$$

where p_{ij} is the transition probability for going from state $\mathbf{A}_i$ to $\mathbf{A}_j$.

From this one-step transition probability matrix, Eq. (23), the N_A-step transition probabilities can be calculated by evaluating $\mathbf{P}^{(N_A)}$ [30]. This matrix contains the probability of being in some given state after N_A transitions have been made. Note that in the current work, a transition corresponds to a deposit attempt. Using Eq. (23), it is then possible to formulate an expression for the expected number of blocks in the deposition window, Eq. (24), after N_A attempts have been made.

$$E_{deposits,N_A} = \sum_{j=1}^{N_{allowed}} \left(\sum_{i=1}^{N_{allowed}} b_i p_{ij}^{(N_A)} \sum_{k=1}^{z} s_{j,k} \right) \tag{24}$$

where $s_{j,k}$ is the k_{th} element of the state $\mathbf{A}_j$, and b_i is the i^{th} element of a vector, $\mathbf{b}$, that holds the initial distribution [31]. In the current work, the process always starts in state $\mathbf{A}_1$. Therefore the distribution is $\mathbf{b} = [\ 1 \quad 0 \quad 0 \quad \cdots \quad 0\ ]$ and Eq. (24) can be reduced to:

$$E_{deposits,N_A} = \sum_{j=1}^{N_{allowed}} \left(p_{1j}^{(N_A)} \sum_{k=1}^{z} s_{j,k} \right) \tag{25}$$

The expected number of failed attempts after N_A attempts is then:

$$E_{failures,N_A} = N_A - E_{deposits,N_A} \tag{26}$$

It can be shown that as $N_A \to \infty$ the probability of being in an absorbing state tends to 1 [32]. The probability that the process ends up in a particular absorbing state can be calculated. To do this, we transform the transition matrix, $\mathbf{P}$, into its canonical form, $\mathbf{P_c}$. This is done by reordering the transition matrix so that the first $n_{absorbing}$ states are absorbing. That is [32],

$$\mathbf{P_c} = \begin{bmatrix} \mathbf{I} & \mathbf{O} \\ \mathbf{R} & \mathbf{Q} \end{bmatrix} \tag{27}$$

where $\mathbf{I}$ is a square $(n_{absorbing} \times n_{absorbing})$ identity matrix and $\mathbf{O}$ is a matrix containing all zeros.

The probability that the process, starting in the transient state $\mathbf{A}_i$, ends up in the absorbing state $\mathbf{A}_j$, is v_{ij}. It can be shown that [32]:

$$\{v_{ij}\} = \mathbf{V} = [\mathbf{I} - \mathbf{Q}]^{-1} \mathbf{R} \tag{28}$$

where $\mathbf{Q}$ and $\mathbf{R}$ are given in Eq. (27).

Using Eq. (28), and given that in the current work the process always starts in the state $\mathbf{A}_1$, it is now possible to give expressions for the expected number of deposits (Eq. (29)) and failed attempts (Eq. (30)) when, in the limit, N_A approaches infinity:

$$E_{deposits,\infty} = \sum_{j \in \Gamma} \left(v_{1j} \sum_{k=1}^{z} s_{j,k} \right) \tag{29}$$

where $\Gamma = \{i \in \mathbb{N} : \mathbf{s}_i \text{ is an absorbing state}\}$, $\mathbb{N}$ is the set of natural numbers.

$$E_{failures,\infty} = N_A - E_{deposits,\infty} \tag{30}$$

4.3.1. A worked example

To understand how the model introduced above can be applied in practice, it is useful to consider a worked example. In this example, a Markov chain will be formulated for a deposition window with $r_1 = 0.6$ m and $r_2 = 0.75$ m. From Eq. (1) and Eq. (2) the corresponding lattice structure has two layers and three disks in each layer.

Starting with this initial knowledge of the lattice structure and using Eq. (19), the following is obtained:

$$\mathbf{G} = \begin{bmatrix} 1/3 \\ 1/3 \end{bmatrix}$$

Let us define some initial state, $\mathbf{A}_1$, to be of the form Eq. (15). Since a trial is assumed to begin with an empty deposition window, the state is given by:

$$\mathbf{A}_1 = \begin{bmatrix} 0 \\ 0 \end{bmatrix}$$

From this initial state, a Markov chain can be constructed by repeated application of Eq. (16) and Eq. (21). Figure 16 shows the Markov chain that is generated through this process. Note that only valid states (with nonzero probability) are shown. Transitions between states represent a new deposit attempt being made.

Using Eq. (25) it is possible to plot the expected number of blocks in the deposition window versus the number of deposit attempts. The expected number of failed attempts to deposit, Eq. (26), can also be plotted. Both of these plots are shown in Figure 17. The shapes of the curves are remarkably similar to those obtained in the simulation (Figure 9). However, it should be noted that the asymptote values are somewhat different. This is due to the approximations made and will be discussed further in Section 4.3.2.

To understand what is happening more clearly, it is insightful to consider the probabilities of the different states in the Markov chain (Figure 16). Table 1 shows that as the number of deposit attempts increases, certain block configurations are more likely to occur. The corresponding states are those that have the outermost layer of the lattice structure complete (no empty disks). This is a general result and extends to all other lattice structures. In the current example, the process will end up in one of the absorbing states: $[\ 1 \quad 3\ ]^T$, $[\ 2 \quad 3\ ]^T$ or $[\ 3 \quad 3\ ]^T$.

From this example, it is clear that there is little to be gained in terms of the total number of blocks deposited by making more than say 10 deposit attempts. This is because the block configuration for the deposition window is not likely to change significantly for deposit attempts beyond this. Even though there may be gaps within the deposition window the states that prevail have a full outermost layer and this prevents robots from accessing, and then making deposits, in the inner layers. This behaviour is a characteristic property of the model. Those block configurations that are more likely to survive with time are those with complete outermost layers.

From Eq. (29) the value towards which the number of deposits converges can be calculated. The

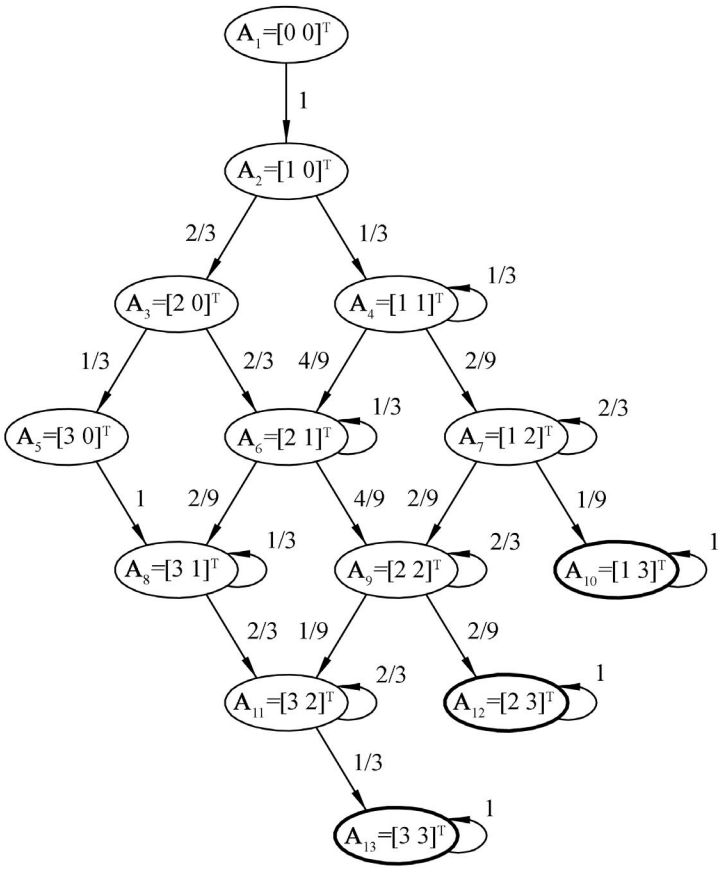

Figure 16. A Markov chain constructed for the worked example in Section 4.3.1. States and the transition probabilities between states are indicated. Absorbing states are emphasised with thicker lines.

canonical transition matrix for the Markov chain in Figure 16 is:

$$\mathbf{P_c} = \begin{array}{c} \\ \mathbf{A_{10}} \\ \mathbf{A_{12}} \\ \mathbf{A_{13}} \\ \mathbf{A_1} \\ \mathbf{A_2} \\ \mathbf{A_3} \\ \mathbf{A_4} \\ \mathbf{A_5} \\ \mathbf{A_6} \\ \mathbf{A_7} \\ \mathbf{A_8} \\ \mathbf{A_9} \\ \mathbf{A_{11}} \end{array} \begin{array}{c} \begin{array}{ccccccccccccc} \mathbf{A_{10}} & \mathbf{A_{12}} & \mathbf{A_{13}} & \mathbf{A_1} & \mathbf{A_2} & \mathbf{A_3} & \mathbf{A_4} & \mathbf{A_5} & \mathbf{A_6} & \mathbf{A_7} & \mathbf{A_8} & \mathbf{A_9} & \mathbf{A_{11}} \end{array} \\ \left[\begin{array}{ccccccccccccc} 1 & 0 & 0 & 0 & 0 & 0 & 0 & 0 & 0 & 0 & 0 & 0 & 0 \\ 0 & 1 & 0 & 0 & 0 & 0 & 0 & 0 & 0 & 0 & 0 & 0 & 0 \\ 0 & 0 & 1 & 0 & 0 & 0 & 0 & 0 & 0 & 0 & 0 & 0 & 0 \\ 0 & 0 & 0 & 0 & 1 & 0 & 0 & 0 & 0 & 0 & 0 & 0 & 0 \\ 0 & 0 & 0 & 0 & 0 & 2/3 & 1/3 & 0 & 0 & 0 & 0 & 0 & 0 \\ 0 & 0 & 0 & 0 & 0 & 0 & 0 & 1/3 & 2/3 & 0 & 0 & 0 & 0 \\ 0 & 0 & 0 & 0 & 0 & 0 & 1/3 & 0 & 4/9 & 2/9 & 0 & 0 & 0 \\ 0 & 0 & 0 & 0 & 0 & 0 & 0 & 0 & 0 & 0 & 1 & 0 & 0 \\ 0 & 0 & 0 & 0 & 0 & 0 & 0 & 0 & 1/3 & 0 & 2/9 & 4/9 & 0 \\ 1/9 & 0 & 0 & 0 & 0 & 0 & 0 & 0 & 0 & 2/3 & 0 & 2/9 & 0 \\ 0 & 0 & 0 & 0 & 0 & 0 & 0 & 0 & 0 & 0 & 1/3 & 0 & 2/3 \\ 0 & 2/9 & 0 & 0 & 0 & 0 & 0 & 0 & 0 & 0 & 0 & 2/3 & 1/9 \\ 0 & 0 & 1/3 & 0 & 0 & 0 & 0 & 0 & 0 & 0 & 0 & 0 & 2/3 \end{array}\right] \end{array}$$

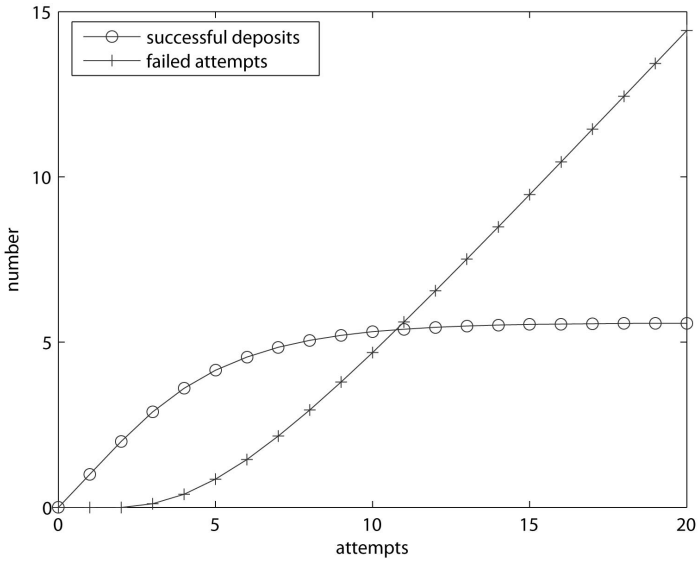

Figure 17. The number of successes and failures versus the number of deposit attempts for the Markov model given in Figure 16.

From Eq. (28), $\mathbf{V}$ can be calculated as:

$$\mathbf{V} = \begin{bmatrix} 0.0370 & 0.3457 & 0.6173 \\ 0.0370 & 0.3457 & 0.6173 \\ 0 & 0.2963 & 0.7037 \\ 0.1111 & 0.4444 & 0.4444 \\ 0 & 0 & 1.0000 \\ 0 & 0.4444 & 0.5556 \\ 0.3333 & 0.4444 & 0.2222 \\ 0 & 0 & 1.0000 \\ 0 & 0.6667 & 0.3333 \\ 0 & 0 & 1.0000 \end{bmatrix}$$

Finally, using the first row from the above result and Eq. (29), it can be calculated that the number of

Table 1. The probabilities of being in the different states of the Markov chain (given in Figure 16) for a varying number of deposit attempts.

State	Number of deposit attempts, N_A														
	0	1	2	3	4	5	6	7	8	9	10	20	30	40	∞
$\mathbf{A}_1 = [0,0]^T$	0	0	0	0	0	0	0	0	0	0	0	0	0	0	0
$\mathbf{A}_2 = [1,0]^T$	1	1	0	0	0	0	0	0	0	0	0	0	0	0	0
$\mathbf{A}_3 = [2,0]^T$	0	0	0.6667	0	0	0	0	0	0	0	0	0	0	0	0
$\mathbf{A}_4 = [1,1]^T$	0	0	0.3333	0.1111	0.0370	0.0123	0.0041	0.0014	0.0005	0.0002	0.0001	0	0	0	0
$\mathbf{A}_5 = [3,0]^T$	0	0	0	0.2222	0	0	0	0	0	0	0	0	0	0	0
$\mathbf{A}_6 = [2,1]^T$	0	0	0	0.5926	0.2469	0.0988	0.0384	0.0146	0.0055	0.0020	0.0007	0	0	0	0
$\mathbf{A}_7 = [1,2]^T$	0	0	0	0.0741	0.0741	0.0576	0.0412	0.0283	0.0192	0.0129	0.0086	0.0002	0	0	0
$\mathbf{A}_8 = [3,1]^T$	0	0	0	0	0.3539	0.1728	0.0796	0.0351	0.0149	0.0062	0.0025	0	0	0	0
$\mathbf{A}_9 = [2,2]^T$	0	0	0	0	0.2798	0.3128	0.2652	0.2030	0.1481	0.1055	0.0741	0.0018	0	0	0
$\mathbf{A}_{10} = [1,3]^T$	0	0	0	0	0.0082	0.0165	0.0229	0.0274	0.0306	0.0327	0.0342	0.0370	0.0370	0.0370	0.0370
$\mathbf{A}_{11} = [3,2]^T$	0	0	0	0	0	0.2670	0.3280	0.3012	0.2467	0.1909	0.1431	0.0051	0.0001	0	0
$\mathbf{A}_{12} = [2,3]^T$	0	0	0	0	0	0.0622	0.1317	0.1906	0.2357	0.2687	0.2921	0.3444	0.3457	0.3457	0.3457
$\mathbf{A}_{13} = [3,3]^T$	0	0	0	0	0	0	0.0890	0.1983	0.2987	0.3810	0.4446	0.6115	0.6171	0.6173	0.6173

deposits made converges towards a value of:

$$\begin{aligned} E_{deposits,\infty} &= (0.0370 \times (1+3)) + (0.3457 \times (2+3)) + (0.6173 \times (3+3)) \\ &= 5.58. \end{aligned}$$

4.3.2. Limits of validity and possible extensions

Figure 18 shows the simulation curves and mathematical model curves for successful deposits for deposition windows of different sizes. The shapes of all the curves are similar. However, there is some difference in the asymptote values between the simulation and mathematical models. As the figure reveals, for values $r_2 \lesssim 0.8$ the mathematical model underestimates (with respect to the simulation result) the asymptote value. Whereas for values of $r_2 \gtrsim 0.8$ the mathematical model overestimates the asymptote value.

The discrepancies are due to the approximations made in formulating the mathematical model. Also, the lattice structure is fitted to the deposition window rather coarsely. Specifically, the deposition process has been modelled as a discrete time Markov chain with a finite number of states. Therefore, the mathematical model is only an approximation of the practical deposition process, where blocks can be deposited at any spatial position within the deposition window (not just at a fixed number of locations in a fixed number of layers), and the deposits are made in continuous rather than discrete time.

While it is beyond the scope of the current work, there may be some benefit in formulating a more general, (continuous) Markov process model, in which blocks can be deposited at any spatial position within the deposition window. This may allow the curves produced by the mathematical model to quantitatively match those produced in simulation. For the current work however, the mathematical model has fulfilled its purpose of allowing analytic expressions to be formulated and a more insightful understanding of the deposition process to be obtained.

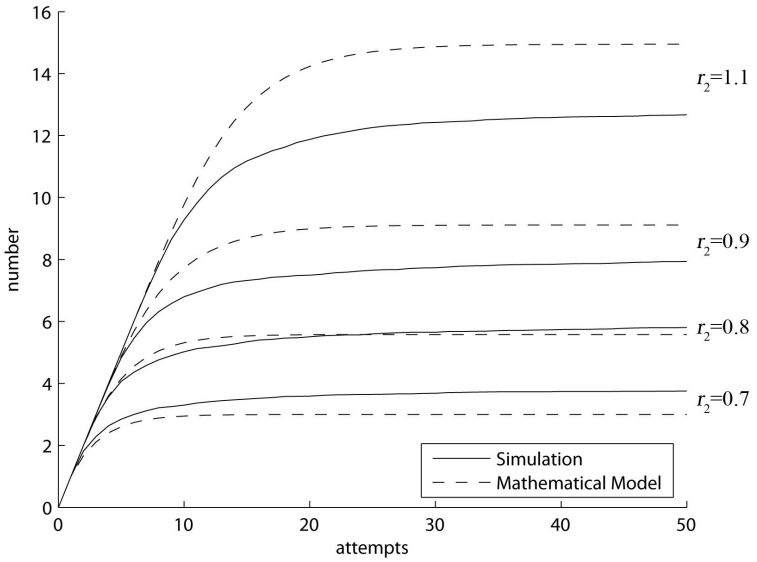

Figure 18. The number of successful deposits versus the number of deposit attempts for different values of r_2 (and keeping $r_1 = 0.6$ m). Results for both simulation and mathematical models are shown.

The primary focus of the paper has been to model a deposition process in which multiple robots interact indirectly through their environment. By adding a block to a deposition window, a builder robot is changing the probability that another (or possibly the same) robot will subsequently be able to make a deposit. The indirect interactions of the swarm are implicitly modelled by considering how the system state is modified when deposits are made by robots. The model does not require the identity of the robot making the deposit to be known, making the model independent of the number of robots present.

It would be useful to consider how the modelling strategy employed in this paper could be extended to other systems with different stigmergic communication schemes (e.g. chemical communication). Markov chain analysis might be a useful tool for predicting and providing a bound on the outcomes of such systems. Modelling the state of the environment that mediates communication, rather than modelling the state of each robot in the swarm, should allow relatively simple models to be formulated that capture the results of complex systems.

A further extension would be to consider the effect of sensor noise, source and sensor non-idealities, imprecise motion and unwanted robot/environment disturbances on the results, and to account for these in the model by modifying the Markov chain transition probabilities. The robustness of the system and the quality of the results obtained could then be assessed under different operating conditions. Applying the modelling strategy to other more complex shapes, in which deposition windows overlap (e.g., [23]), may also be useful.

5. Discussion and Conclusion

In this paper, simulation and mathematical models have been developed to give a deeper understanding of a collective construction deposition process. The models are based upon the deposition behaviour of real robots and produce results that are similar to those observed in practice. Both models account for the internal cavities observed in the deposited block patterns within practical deposition windows. They also predict the dynamics observed in practical trials, explaining why the chance of failure increases with each new deposit attempt made.

As the models reveal, the number of failed deposit attempts can serve to indicate the state of a deposition window. By accessing this information through a distributed feedback mechanism, the swarm is able to regulate construction. Specifically, builder robots produce a flash signal when they fail on two consecutive attempts to deposit (rule 4, Rule Set 2). By counting these flash signals from possibly different robots, the organiser robot is acquiring information related to the number of failed attempts and, therefore, the number of deposits made. It is then in a position to make an informed decision as to when the current deposition window should be deemed complete and a new deposition window created. Practically, this is done through an appropriate setting of the *flash_count_max* parameter (see rule 2, Rule Set 1).

It is clear that the minimalism of the robot swarm is due, in part, to the robots' ability to extract and use relatively complex information encoded into the environment. The feedback system discussed above is evidence of this, with the robots obtaining information about their task progress from the structure being built. The template used provides another source of environmental information. Builder robots 'unlock' the quantitative information contained in the template and use it to guide them where to deposit. In both of the aforementioned cases the information used by the robots has a spatial relevance. That is, the information is contained at a location in the environment where it is actually needed.

Rather than using an organiser robot equipped with a light source to create a template, it would be interesting to investigate how physical templates created by self-organising swarm members might be used

instead. In a manner similar to the ants, *Leptothorax albipennis*, that build their nest walls a certain distance from a cluster of brood/adult ants [33, 34], the size and distribution of a gathering of robots could be used as a template to guide construction. In this way, dependence on a single organiser robot could be removed and the robustness of the swarm system enhanced, since the loss of a single robot would not imply the loss of the template. A very interesting avenue for future research would be to investigate how spatio-temporal varying physical templates could be implemented in this context.

For the future, the development of additional swarm systems (and their associated models) is needed to better understand how information sources contained in the environment can be used by robots. Here, social insects will likely provide us with a plethora of excellent examples [35]. When environmental information is accessible and reliable, it allows the environment to be considered "as an external memory resource" [36]. From an engineering perspective, the environment can then be thought of as storing physically embodied code, dynamically programmed and executed by robots. By allowing the complexity of these physically embodied programs to grow with time, robots may be able to perform very difficult spatio-temporal tasks whilst still remaining minimalist in their design.

Acknowledgments

The authors gratefully acknowledge the support of the Australian Research Council funded Centre for Perceptive and Intelligent Machines in Complex Environments. The work has also been supported by a grant from Monash University's Faculty of Engineering Small Grants Scheme.

References

[1] W. M. Wheeler, *The Social Insects: Their Origin and Evolution*, London, Kegan Paul, Trench, Trubner and Co., Ltd., 1928.

[2] E. O. Wilson, *Insect Societies*, Cambridge, MA, The Belknap Press of Harvard University Press, 1974.

[3] E. Bonabeau, M. Dorigo, G. Theraulaz, *Swarm Intelligence: From Natural to Artificial Systems*, NY, Oxford University Press, 1999.

[4] M. Dorigo, E. Şahin, "Guest editorial," *Autonomous Robots*, Vol. 17, pp. 111–113, 2004.

[5] R. L. Stewart, *Construction with a Swarm of Minimalist Robots using Templates and Feedback*, PhD thesis, Monash University, 2006.

[6] A. J. Ijspeert, A. Martinoli, A. Billard, L. M. Gambardella, "Collaboration through the exploitation of local interactions in autonomous collective robotics: the stick pulling experiment," *Autonomous Robots*, Vol. 11, pp. 149–171, 2001.

[7] A. Martinoli, A. J. Ijspeert, F. Mondada, "Understanding collective aggregation mechanisms: From probabilistic modelling to experiments with real robots," *Robotics and Autonomous Systems*, Vol. 29, pp. 51–63, 1999.

[8] A. Martinoli, A. J. Ijspeert, L. M. Gambardella, "A probabilistic model for understanding and comparing collective aggregation mechanisms," in D. Floreano, J.-D. Nicoud, F. Mondada, eds., *Advances in Artificial Life: 5th European Conference, ECAL99, Lausanne, Switzerland, September 13-17, 1999. Proceedings*, Vol. 1674 of *Lecture Notes in Artificial Intelligence (Subseries of Lecture Notes in Computer Science)*, pp. 575–584, NY, Springer-Verlag, 1999.

[9] C. A. C. Parker, H. Zhang, C. Ronald Kube, "Blind bulldozing: Multiple robot nest construction," in *Proc. of the 2003 IEEE/RSJ International Conference on Intelligent Robots and Systems (IROS'03)*, pp. 2010–2015, 2003.

[10] W. M. Spears, D. F. Spears, J. C. Hamann, R. Heil, "Distributed, physics-based control of swarms of vehicles," *Autonomous Robots*, Vol. 17, pp. 137–162, 2004.

[11] G. Theraulaz, E. Bonabeau, "Modelling the collective building of complex architectures in social insects with lattice swarms," *Journal of Theoretical Biology*, Vol. 177, pp. 381–400, 1995.

[12] C. Melhuish, J. Welsby, C. Edwards, "Using templates for defensive wall building with autonomous mobile ant-like robots," in *Proc. of Towards Intelligent Mobile Robots (TIMR'99)*, 1999.

[13] J. Wawerla, G. S. Sukhatme, M. J. Matarić, "Collective construction with multiple robots," in *Proc. of the 2002 IEEE/RSJ International Conference on Intelligent Robots and Systems (IROS'02)*, pp. 2696–2701, 2002.

[14] J. K. Werfel, "Building blocks for multi-robot construction," in *Proc. of the 7th International Symposium on Distributed Autonomous Robotic Systems (DARS'04)*, 2004.

[15] E. O. Wilson, *Sociobiology: The New Synthesis*, Cambridge, MA, The Belknap Press of Harvard University Press, 1975.

[16] P.-P. Grassé, "La reconstruction du nid et les coordinations interindividuelles chez *Bellicositermes Natalensis* et *Cubitermes Sp.* la théorie de la stigmergie: Essai d'interprétation du comportement des termites constructeurs," *Insectes Sociaux*, Vol. 6, pp. 41–80, 1959.

[17] C. Jones, M. J. Matarić, "From local to global behavior in intelligent self-assembly," in *Proc. of the 2003 IEEE International Conference on Robotics and Automation (ICRA'03)*, pp. 721–726, 2003.

[18] G. Li, H. Zhang, "A rectangular partition algorithm for planar self-assembly," in *Proc. of the 2005 IEEE/RSJ International Conference on Intelligent Robots and Systems (IROS'05)*, pp. 3213–3218, 2005.

[19] J. Bishop, S. Burden, E. Klavins, R. Kreisberg, W. Malone, N. Napp, T. Nguyen, "Programmable parts: a demonstration of the grammatical approach to self-organization," in *Proc. of the 2005 IEEE/RSJ International Conference on Intelligent Robots and Systems (IROS'05)*, pp. 3684–3691, 2005.

[20] J. K. Werfel, Y. Bar-Yam, R. Nagpal, "Building patterned structures with robot swarms," in *Proc. of the 19th International Joint Conference on Artificial Intelligence (IJCAI'05)*, pp. 1495–1502, 2005.

[21] R. L. Stewart, R. A. Russell, "Emergent structures built by a minimalist autonomous robot using a swarm-inspired template mechanism," in *Proc. of the First Australian Conference on Artificial Life (ACAL'03)*, pp. 216–230, 2003.

[22] R. L. Stewart, R. A. Russell, "Building a loose wall structure with a robotic swarm using a spatio-temporal varying template," in *Proc. of the 2004 IEEE/RSJ International Conference on Intelligent Robots and Systems (IROS'04)*, pp. 712–716, 2004.

[23] R. L. Stewart, R. A. Russell, "A generalised technique for building 2D structures with robot swarms," in H. A. Abbass, T. Bossomaier, J. Wiles, eds., *Recent Advances in Artificial Life - Advances in Natural Computation - Vol. 3*, pp. 265–277, Singapore, World Scientific Publishing Co. Pte. Ltd, 2005.

[24] R. L. Stewart, R. A. Russell, "A distributed feedback mechanism to regulate wall construction by a robotic swarm," *Adaptive Behavior*, Vol. 14, pp. 21–51, 2006.

[25] O. H. Bruinsma, *An Analysis of Building Behaviour of the Termite* Macrotermes subhyalinus *(Rambur)*, PhD thesis, The Netherlands, Landbouwhogeschool te Wageningen, 1979.

[26] G. Theraulaz, E. Bonabeau, J.-L. Deneubourg, "The mechanisms and rules of coordinated building in social insects," in C. Detrain, J.-L. Deneubourg, J. M. Pasteels, eds., *Information Processing in Social Insects*, pp. 309–330, Basel, Switzerland, Birkhäuser Verlag, 1999.

[27] R. A. Brooks, "A robust layered control system for a mobile robot," *IEEE Journal of Robotics and Automation*, Vol. 2, pp. 14–23, 1986.

[28] J. H. Conway, N. J. A. Sloane, *Sphere Packings, Lattices and Groups*, NY, Springer-Verlag, 1988.

[29] A. Ostebee, P. Zorn, *Multivariable Calculus from Graphical, Numerical, and Symbolic Points of View*, Fort Worth, Saunders College Publishing, Harcourt Brace College Publishers, (revised preliminary edition), 1998.

[30] S. M. Ross, *Introduction to Probability Models*, San Diego, Academic Press, 6th edition, 1997.

[31] W. Feller, *An Introduction to Probability Theory and its Applications*, Vol. I, NY, John Wiley and Sons, Inc., 3rd edition, 1968.

[32] J. G. Kemeny, J. L. Snell, *Finite Markov Chains*, NY, Springer-Verlag, 1983.

[33] N. R. Franks, A. Wilby, B. W. Silverman, C. Tofts, "Self-organizing nest construction in ants: sophisticated building by blind bulldozing," *Animal Behaviour*, Vol. 44, pp. 357–375, 1992.

[34] N. R. Franks and J.-L. Deneubourg, "Self-organizing nest construction in ants: individual worker behaviour and the nest's dynamics," *Animal Behaviour*, Vol. 54, pp. 779–796, 1997.

[35] C. Detrain, J.-L. Deneubourg, J. M. Pasteels, eds., *Information Processing in Social Insects*, Basel, Switzerland, Birkhäuser Verlag, 1999.

[36] R. Beckers, O. E. Holland, J.-L. Deneubourg. "From local actions to global tasks: stigmergy and collective robotics," in R. A. Brooks, P. Maes, eds., *Artificial Life IV: Proceedings of the Fourth International Workshop on the Synthesis and Simulation of Living Systems*, pp. 181–189, Cambridge, MA, MIT Press, 1994.